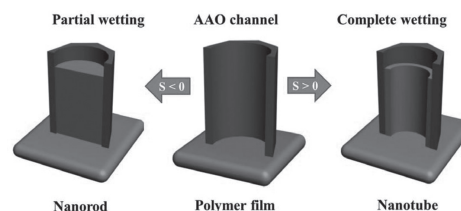


# Solvent-Annealing-Induced Nanowetting in Templates: Towards Tailored Polymer Nanostructures

Jiun-Tai Chen,\* Chih-Wei Lee, Mu-Huan Chi, I-Chun Yao

We study the solvent-annealing-induced nanowetting in templates using porous anodic aluminum oxide membranes. The morphology of polystyrene and poly(methyl methacrylate) nanostructures can be controlled, depending on whether the swollen polymers are in the partial or complete wetting regimes, which are characterized by the spreading coefficient. When the swollen polymers are in the partial wetting regime, polymers wet the nanopores by capillary action, resulting in the formation of polymer nanorods. When the swollen polymers are in the complete wetting regime, polymers form wetting layers in the nanopores, resulting in the formation of polymer nanotubes. The solubility parameters of polymers and solvents are also used to predict the wetting behavior of swollen polymers in cylindrical geometry.



## 1. Introduction

Polymer nanostructures have attracted great attention in recent years because of their significance in both basic science and practical applications.<sup>[1,2]</sup> Polymer nanostructures have been applied to diverse areas such as sensors, drug delivery, tissue engineering, and organic solar cells.<sup>[3–6]</sup> One of the common methods to prepare polymer nanostructures is the template method, in which polymer melts or solutions are introduced to the nanopores of a porous template by wetting.<sup>[7–16]</sup> After the polymers are solidified in the nanopores, polymer nanostructures can be obtained after the porous template is selectively removed.<sup>[15]</sup> A major advantage of the template method is that the dimensions of the polymer nanostructures can be controlled by the sizes of the nanopores of the templates. Various polymer nanostructures have been prepared in the past, and properties and morphologies which are not present in the bulk are observed.<sup>[17,18]</sup>

Two main wetting-based techniques have been used to prepare polymer nanostructures by using porous templates such as the anodic aluminum oxide (AAO)

template. These two techniques are the solution method and the melt method.<sup>[15]</sup> In the solution method, polymers are first dissolved in a suitable solvent.<sup>[19]</sup> Then, the polymer solution is introduced into the nanopores of templates by capillary force. Polymer nanotubes are usually observed by using the solution method because of the adsorption of the polymer chains on the pore walls of the porous templates. The wall thickness of the polymer nanotubes can be controlled by the polymer concentration.<sup>[20,21]</sup> Wendorff et al.<sup>[22]</sup> studied the effect of polymer molecular weight on the formation of polystyrene (PS) nanostructures by wetting AAO templates with PS solution. Feng and Jin<sup>[23]</sup> also studied the effect of interfacial interactions on controlling the morphologies of polymer nanostructures by using solvents which have preferential affinity to alumina walls.

The second wetting-based technique to prepare polymer nanostructures using porous templates is the melt method. In this method, polymer powders or films are brought into contact with the nanopores of the porous templates, and no solvent is involved in the wetting process.<sup>[24]</sup> After the samples are annealed above the glass transition temperatures or the melting temperatures of the polymers, polymer chains wet the pore walls of the templates. Steinhart et al.<sup>[25]</sup> pioneered this method by placing polymers on pore arrays at temperatures above the glass transition temperatures or the melting

Prof. J.-T. Chen, C.-W. Lee, M.-H. Chi, I.-C. Yao  
Department of Applied Chemistry, National Chiao Tung  
University, Hsinchu, Taiwan 30050  
E-mail: jtchen@mail.nctu.edu.tw

temperatures. Amorphous or semicrystalline polymer nanotubes can be prepared by this method. Russell and coworkers<sup>[26]</sup> later studied the wetting transition of polymers with different molecular weights using the melt method.

Although the solution method and the melt method are widely used in fabricating different polymer nanostructures, there are still some disadvantages by using these two methods. For the solution method, one disadvantage is that there are usually unnecessary polymer films outside the nanopores of the templates after the evaporation of the solvent. Removing such polymer films outside the nanopores is usually problematic. The main disadvantage of using the melt method is that polymers may thermally degrade or decompose after high-temperature annealing. Therefore, the properties of the polymer nanostructures are affected, and the applications of these nanostructures are limited.

To overcome the limitations of these two methods, Ho et al.<sup>[27]</sup> recently studied the solvent annealing method to fabricate carbon tubes by carbonizing poly(acrylonitrile) (PAN) nanotubes. Although polymer nanotubes can be prepared, the formation mechanism and the effect of the annealing solvent on the morphologies of the resultant polymer nanostructures are still not clear. To further study the formation mechanism of polymer nanostructures by the solvent-annealing-induced nanowetting in templates (SAINT), we investigate the wetting behavior of polymer films in cylindrical AAO pores using different annealing solvents. We find that the morphologies of polymer nanostructures prepared by SAINT are determined by the wetting regimes in the cylindrical nanopores.

The wetting regimes of the swollen polymers in the cylindrical nanopores are characterized by the spreading coefficient ( $S$ ). Similar to the case of a non-volatile liquid wetting on a flat substrate, the spreading coefficient is described as

$$S = \gamma_{SG} - \gamma_{SL} - \gamma \quad (1)$$

where  $\gamma_{SG}$  is the interfacial tension between the solid and the gas,  $\gamma_{SL}$  is the interfacial tension between the solid and the liquid, and  $\gamma$  is the interfacial tension between the liquid and the gas.<sup>[28]</sup>  $S$  is the energy difference between the bare and wet substrates. If  $S > 0$ , the liquid is in the complete wetting regime. The liquid on a solid substrate spreads spontaneously and forms a layer of liquid film. The thickness of the liquid film results from the competition between long-range forces.<sup>[29]</sup> In the complete wetting regime, the swollen polymer forms a wetting layer on the pore walls of the templates, resulting in the formation of polymer nanotubes. If  $S < 0$ , the liquid is in the partial wetting regime. The liquid on a solid substrate spreads and reaches an equilibrium shape with a contact angle  $\theta_E$ , which is given by the Young's law:<sup>[30]</sup>

$$\theta_E = \cos^{-1}(\gamma_{SG} - \gamma_{SL})/\gamma \quad (2)$$

In the partial wetting regime, the swollen polymer wets the cylindrical nanopores by capillary action, resulting in the formation of polymer nanorods.

## 2. Experimental Section

### 2.1. Materials

Poly(methyl methacrylate) (PMMA;  $\bar{M}_n = 60\,000$ ;  $\bar{M}_w = 68\,500$ ; PDI = 1.14) was purchased from Polymer Source Inc. Polystyrene (PS;  $\bar{M}_n = 58\,000$ ;  $\bar{M}_w = 86\,000$ ; PDI = 1.48) was purchased from Sigma-Aldrich. *N,N*-Dimethyl-formamide (DMF), tetrahydrofuran (THF), toluene, acetone, and benzene were obtained from TEDIA. The AAO templates (pore diameter  $\approx 150$ – $400$  nm, thickness  $\approx 60$   $\mu\text{m}$ ) were obtained from Whatman. Sodium hydroxide (NaOH) was purchased from TEDIA. Polycarbonate filters (VCTP, pore size: 0.1  $\mu\text{m}$ ) were obtained from Millipore. The glass substrates were purchased from the FEA Company, with the length, width, and thickness of 76, 26, and 1.2 mm, respectively. The glass slides were cleaned with acetone before use.

### 2.2. Fabrication of Polymer Nanostructures

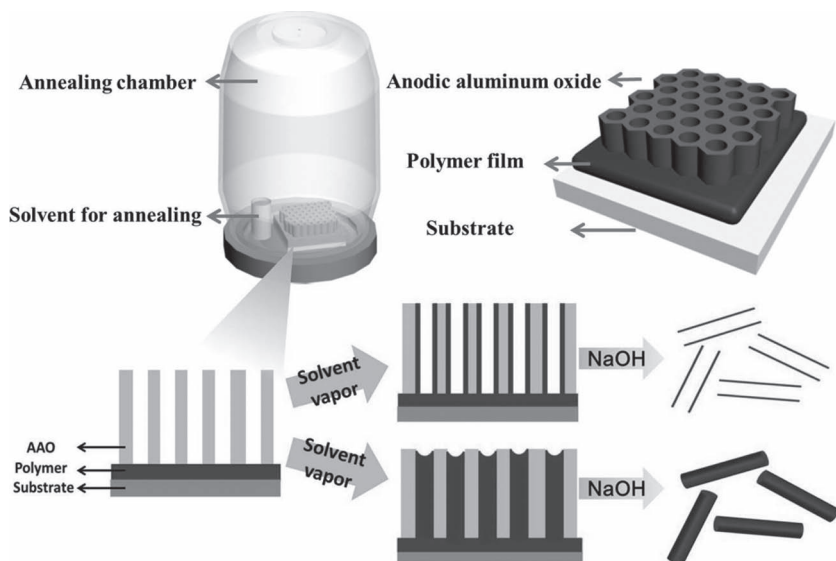
PMMA and PS nanostructures were prepared under similar conditions. To prepare PMMA nanostructures, for example, a PMMA film was first made by spin-coating a 10 wt% solution (PMMA in THF) at 2000 rpm for 60 s. An AAO template was then placed on top of the PMMA film. Subsequently, the sample was placed in a chamber, which contains an open bottle of the annealing solvent. After the solvent annealing process for 2 d, the samples were taken out from the annealing chamber. The sample was dried with a vacuum pump and immersed into 5 wt% NaOH<sub>(aq)</sub> to selectively remove the AAO template. Finally, the sample was filtered and washed with deionized water using a polycarbonate filter.

### 2.3. Structure Analysis and Characterization

A scanning electron microscope (SEM) (JEOL JSM-7401F) with an accelerating voltage of 10 kV was used to investigate the polymer nanostructures. Before the SEM measurement, the samples were dried at 30 °C in a vacuum oven and coated with 4 nm platinum. A transmission electron microscope (TEM) (JEOL JEM-2010) with an accelerating voltage of 200 kV was also used. Before the TEM measurement, the samples were placed onto copper grids coated with carbon or Formvar.

## 3. Results and Discussion

Two commonly used polymers, polystyrene and poly(methyl methacrylate) are used in this work. Scheme 1 shows the schematic illustration of the experimental process to prepare polymer nanostructures using



**Scheme 1.** Schematic illustration of the experimental process to prepare polymer nanostructures by SAINT. An AAO template was placed on top of a spin-coated polymer film. During the solvent annealing process, polymer chains wet the cylindrical pores of the AAO templates. After the AAO template is selectively removed by  $\text{NaOH}_{(\text{aq})}$ , polymer nanorods or nanotubes are obtained, depending on the type of the annealing solvent.

SAINT. At first, a polymer film is spin-coated onto a glass substrate. The polymer film is then dried to ensure that no residual solvent is present in the polymer film. If the polymer films are not dried before the annealing process, polymer patterns on the polymer film surface are immediately formed once the films are in contact with the template, similar to the micromolding process. Then, the polymer film coated on the substrate is brought into contact with the AAO template. The sample is placed in a solvent-annealing chamber, and the wetting process is performed for the desired length of time. Subsequently, the sample is taken out from the annealing chamber and is dried under vacuum to remove the residual solvent. After the AAO template is selectively removed by  $\text{NaOH}_{(\text{aq})}$ , polymer nanorods or nanotubes are obtained, depending on the type of the annealing solvent. If the solvent is not dried completely before immersing the sample into  $\text{NaOH}$  solution, water in the solution may cause morphology changes of the resultant polymer nanostructures.<sup>[31]</sup>

The porous templates used for wetting experiments usually have high surface energy and are wettable by liquid with low surface energy such as polymers. Anodic aluminum oxide (AAO) is often used as templates for making polymer nanostructures because of the high pore density, the regular pore size distribution, and the high aspect ratio of the cylindrical pores.<sup>[32]</sup> In this work, we choose AAO membranes as the templates, and the average pore size of the AAO template is  $\approx 237$  nm.<sup>[31]</sup>

In the SAINT process, polymer films with uniform thickness are prepared by spin coating to ensure a good

contact between the polymer film and the AAO template. Chen et al.<sup>[33]</sup> studied the wetting of polymer microspheres into the nanopores of the AAO templates by thermal annealing. At the beginning of the wetting process, only a limited area of the microsphere is in contact with the template. With time, polymers are drawn into the nanopores, and more of the microspheres comes into contact with the template, causing a distribution of the length of the nanorods in the AAO template.<sup>[33]</sup>

The wetting experiment is first performed for PMMA by annealing PMMA films in the vapors of different solvents. Figure 1 shows the SEM and TEM images of PMMA ( $\overline{M}_w$ :  $68.5$  kg mol<sup>-1</sup>) nanotubes and nanorods prepared by SAINT. When the PMMA film is annealed in a toluene vapor for 2 d, PMMA nanotubes are obtained, as shown in Figure 1a and b. The open ends of the PMMA nanotubes can be seen from the SEM image

(Figure 1a). The top parts of the PMMA nanotubes are connected because the polymers have reached the top of the AAO template and wet the top surface of the template. To further confirm the hollow nature of the polymer nanotubes, TEM is also performed. As shown in the TEM image (Figure 1b), a PMMA nanotube with a diameter of  $\approx 220$  nm and a wall thickness of  $\approx 50$  nm is observed.

When the PMMA film is annealed in a DMF vapor for 2 d, PMMA nanorods are obtained, as shown in Figure 1c and d for the SEM and TEM images, respectively. In the SEM image, the top surfaces of the nanorods appear darker, showing the depressions in the center of the top ends of the nanorods. Such depressions indicate the signature of the meniscus of the swollen polymers during the wetting process.<sup>[34]</sup> The meniscus of nanorods can sometimes be wrongly interpreted as nanotubes by analyzing the SEM images. Therefore, TEM measurements are performed to confirm the solid nature of the nanorods, as shown in Figure 1d. Three other solvents including benzene, THF, and acetone are also used as the annealing solvents. PMMA nanotubes are obtained by annealing PMMA films using these three solvents, as shown in the Supporting Information.

In addition to PMMA, another commonly used polymer, PS, is also studied for the SAINT method. PS has a weaker interaction with the pore walls of the AAO template than PMMA does, because of the lower polarity of the functional group in PS. Additionally, the surface tension of PS ( $\gamma = 40.7$  dyn cm<sup>-1</sup> at 20 °C) is slightly lower than that of PMMA ( $\gamma = 41.1$  dyn cm<sup>-1</sup> at 20 °C). Figure 2 shows the

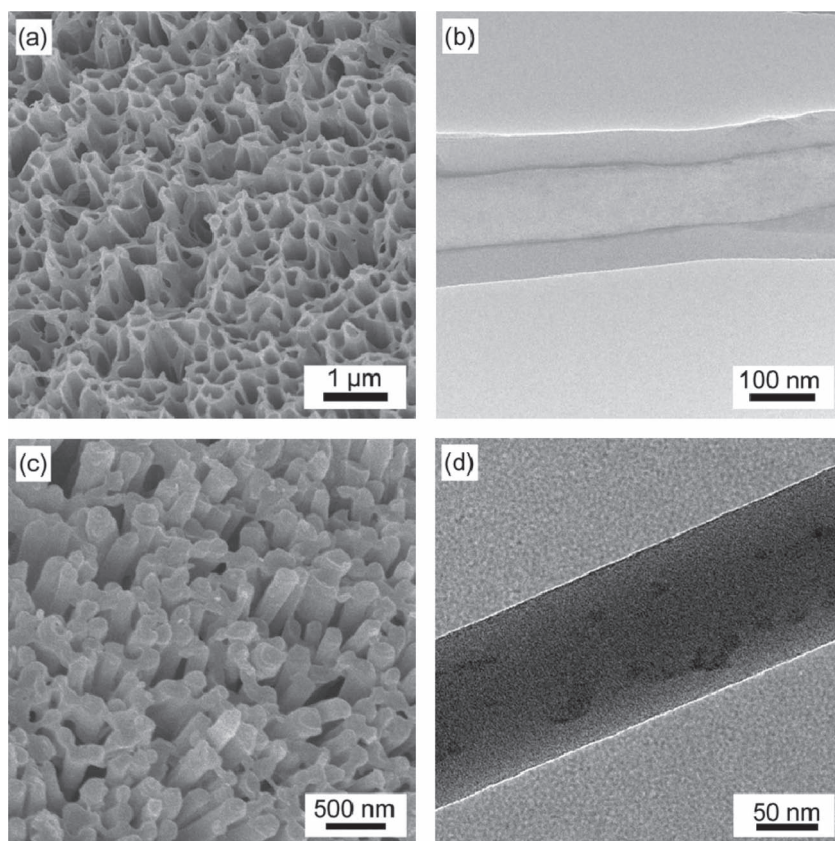


**Figure 1.** SEM and TEM images of PMMA ( $\bar{M}_w$ : 68.5 kg mol<sup>-1</sup>) nanotubes and nanorods. PMMA nanotubes are obtained by annealing a PMMA film in a toluene vapor for 2 d. PMMA nanorods are obtained by annealing a PMMA film in a DMF vapor for 2 d. (a) SEM image of PMMA nanotubes. (b) TEM image of a PMMA nanotube. (c) SEM image of PMMA nanorods. (d) TEM image of a PMMA nanorod.

Figure S3 (Supporting Information) shows the plot of the length of PMMA ( $\bar{M}_w$ : 68.5 kg mol<sup>-1</sup>) nanotubes versus the time of the wetting process. The PMMA films are annealed in THF vapor, and the length of the PMMA nanotubes increases with the wetting time. At the beginning of the solvent annealing process, the annealing chamber is not saturated with solvent vapors. Therefore, the initial growth rate of the nanotubes is slower than that at longer annealing times, resulting in the non-linear relationship between the length of nanotubes and the annealing time.

The proposed mechanism of forming the polymer nanorods and nanotubes by SAINT is shown in Figure 3. When the swollen polymers are in the partial wetting regime,  $S$  is smaller than zero, and the swollen polymers wet the nanopores by capillary action. After the evaporation of the solvent, polymer nanorods are formed. The sizes of the nanorods are smaller than the sizes of the pores of the AAO template because of the shrinkage towards to the pore walls. When the swollen polymers are in the complete wetting regime,  $S$  is larger than zero, and the swollen polymers form wetting films on the pore walls. After evaporation of the solvent, polymer nanotubes are formed. The

SEM and TEM images of PS nanostructures prepared by SAINT using different solvents. PS nanorods are obtained by annealing a PS film in an acetone vapor for 2 d, while PS nanotubes are obtained when the PS film is annealed in a benzene vapor. Therefore, similar to PMMA, the morphology of PS nanostructures can also be controlled by using different solvents in the SAINT process. Three other solvents including DMF, THF, and benzene are also used as the annealing solvents. PS nanorods are obtained by annealing PS films in a vapor of DMF, while PS nanotubes are obtained when the films are annealed in vapors of THF or toluene, as shown in the Supporting Information.

In the partial wetting region, swollen polymers wet the cylindrical pores by capillary force. The capillary force originates from the reduction of the interfacial energy by replacing the interface of air/alumina wall with the interface of polymer/alumina.

The time of the wetting process is also studied. In the complete wetting regime, more swollen polymers wet the wall surfaces with longer annealing time, resulting in the formation of longer polymer nanotubes.

wall thickness of the nanotubes by solvent annealing is smaller than the thickness of the wetting layer of the swollen polymers.

In the SAINT process, the polymer films are annealed under the AAO template. To evaluate whether the wetting process is affected by the gravity, the capillary length ( $\kappa^{-1}$ ) is considered. The capillary length is defined as

$$\kappa^{-1} = (\gamma/\rho g)^{1/2} \quad (3)$$

where  $\gamma$  is the surface tension,  $\rho$  is the density, and  $g$  is the gravity.<sup>[35]</sup> Gravitational effect is negligible when the size is smaller than the capillary length. Since the pore diameters of the AAO template ( $\approx 200$  nm) are much smaller than the capillary length of the swollen polymers, which is in the millimeter range, the gravitational effect is negligible in this study. Consequently, the same results are obtained whether the polymer films are placed under or above the AAO templates.

Previously, Russell and coworkers<sup>[36,37]</sup> studied that polymer nanotubes prepared by the solution wetting

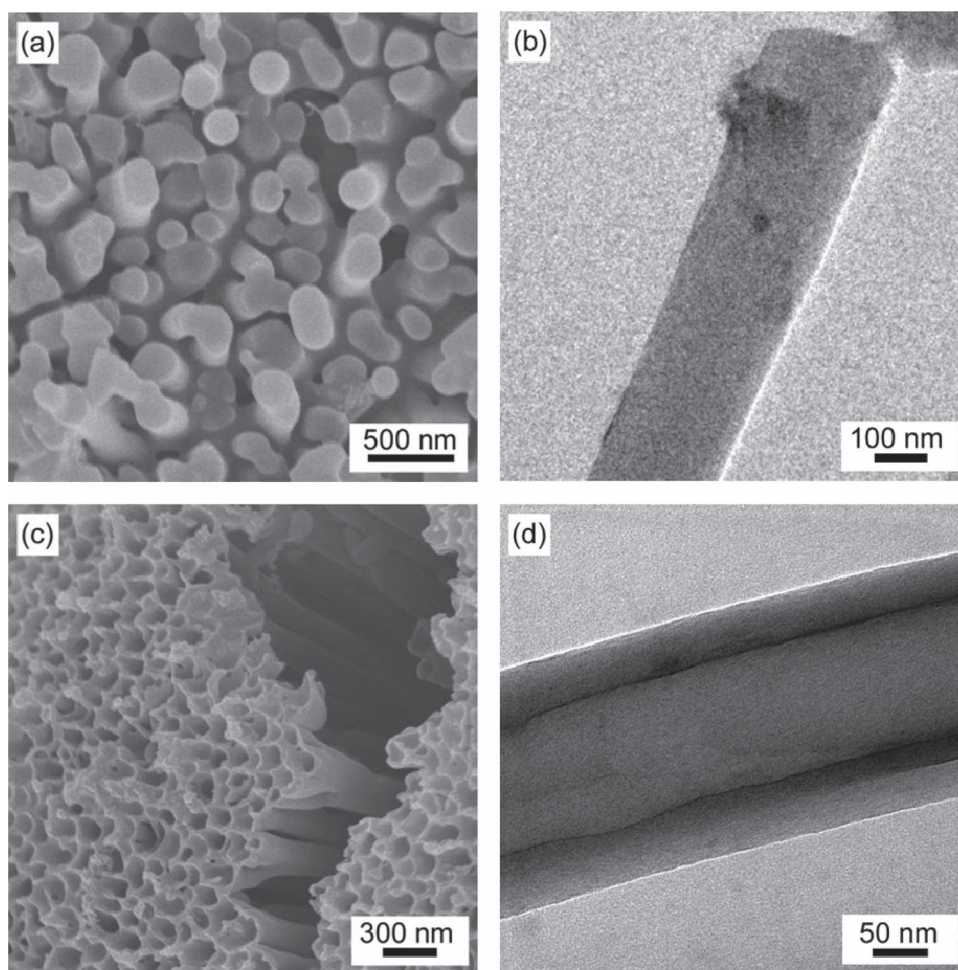


**Figure 2.** SEM and TEM images of PS ( $\overline{M}_w$ : 86 kg/mol) nanorods and nanotubes. PS nanorods are obtained by annealing a PS film in an acetone vapor for two days. PS nanotubes are obtained by annealing a PS film in a benzene vapor for 2 d. (a) SEM image of PS nanorods. (b) TEM image of a PS nanorod. (c) SEM image of PS nanotubes. (d) TEM image of a PS nanotube.

method can undergo morphology transformation upon thermal annealing, driven by the Rayleigh instability. The surface of polymer film confined in the cylindrical nanopores undulates with a finite wavelength to reduce the surface area. With time the undulation grows in amplitude and eventually bridges together, and polymer nanorods with periodic encapsulated holes are formed. This type of instability, however, is not observed during the wetting process when the swollen polymer wets the pores in the complete wetting regime. The instability is expected to occur when polymer nanotubes prepared by SAINT are post-treated by thermal annealing.

This work studies the wetting by using different annealing solvents. To further examine the effect of annealing solvent on the formation of polymer nanostructures, we compare the Hildebrand solubility parameters ( $\delta$ ) of the polymers and solvents. The Hildebrand solubility parameters are often used to predict the solubility and swelling of polymers by solvents and are defined as the square root of the cohesive energy density.<sup>[38]</sup>

Table 1 shows the summary table of the solubility parameters of polymers and solvents and resultant polymer nanostructures. Polymers are more soluble in solvents with similar values of solubility parameters. We find that polymer nanotubes are formed when the differences of the solubility parameters between polymers and solvents are small ( $\Delta\delta \leq 0.6(\text{cal cm}^{-3})^{1/2}$ ). When the differences of the solubility parameters are large ( $\Delta\delta \geq 0.77(\text{cal cm}^{-3})^{1/2}$ ), polymer nanorods are formed.

The results of SAINT are also compared to the results of thermally induced wetting, as demonstrated by Russell and coworkers.<sup>[26]</sup> As shown in the Supporting information, nanorods and nanotubes can be made by controlling the temperatures of thermally induced wetting. For example, PS ( $\overline{M}_w$ : 86 kg mol<sup>-1</sup>) nanorods are obtained by thermally annealing a PS film at 120 °C, while PS nanotubes are obtained by thermally annealing a PS film at 210 °C (see Figure S4, Supporting Information). Therefore, the concept of different wetting regimes in cylindrical pores by thermal annealing is similar to the concept of

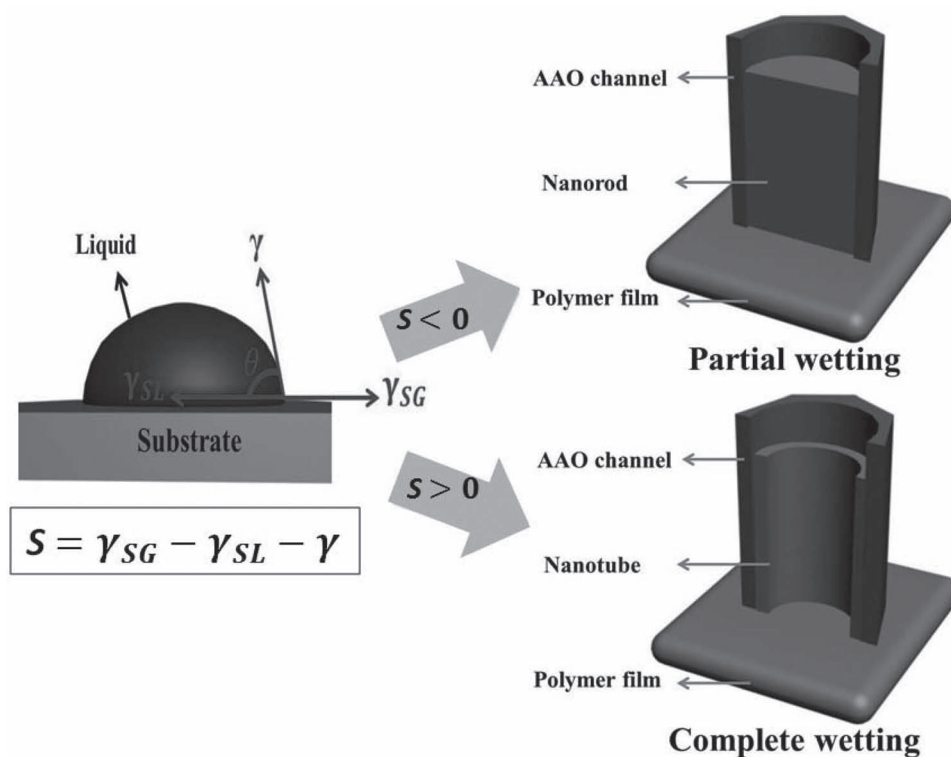


**Figure 3.** The formation mechanism of polymer nanorods or nanotubes by SAINT. Nanorods are generated when  $S < 0$  (partial wetting), and nanotubes are generated when  $S > 0$  (complete wetting).

**Table 1.** A summary table of the solubility parameters of polymers and solvents and resultant polymer nanostructures.

Solubility parameter ( $\delta$ ) ( $\text{cal cm}^{-3}$ ) <sup>1/2</sup>	DMF ( $\delta = 12.1$ )	Acetone ( $\delta = 9.9$ )	Toluene ( $\delta = 8.9$ )	THF ( $\delta = 9.1$ )	Benzene ( $\delta = 9.2$ )
PMMA ( $\delta = 9.3$ )	Nanorods ( $\Delta\delta = 2.8$ )	Nanotubes ( $\Delta\delta = 0.6$ )	Nanotubes ( $\Delta\delta = 0.4$ )	Nanotubes ( $\Delta\delta = 0.2$ )	Nanotubes ( $\Delta\delta = 0.1$ )
PS ( $\delta = 9.13$ )	Nanorods ( $\Delta\delta = 2.97$ )	Nanorods ( $\Delta\delta = 0.77$ )	Nanotubes ( $\Delta\delta = 0.23$ )	Nanotubes ( $\Delta\delta = 0.03$ )	Nanotubes ( $\Delta\delta = 0.07$ )

different wetting regimes induced by different solvents, as we demonstrate here.

be applied to other functional materials such as metals or inorganic materials.

## 4. Conclusion

We study the fabrication of polymer nanostructures by using the SAINT. The elevation of temperature is not required during the wetting process, and the degradation problem of the melt wetting method is avoided. In the wetting process, polymer nanorods or nanotubes can be fabricated, depending on whether the swollen polymers are in the partial or complete wetting regimes, which are characterized by the spreading coefficient ( $S$ ). The length of the nanotubes can also be controlled by controlling the wetting time. This innovative study opens a new branch of investigation in the field of template-based polymer nanostructures. In addition to polymers, SAINT can also

## Supporting Information

Supporting Information is available from the Wiley Online Library or from the author.

Acknowledgements: This work was supported by the National Science Council.

Received: September 25, 2012; Revised: October 31, 2012; Published online: December 12, 2012; DOI: 10.1002/marc.201200640

Keywords: nanotubes; nanorods; solvent annealing; templates; wetting

- [1] H. D. Tran, D. Li, R. B. Kaner, *Adv. Mater.* **2009**, *21*, 1487.
- [2] Y. Z. Long, M. M. Li, C. Z. Gu, M. X. Wan, J. L. Duvail, Z. W. Liu, Z. Y. Fan, *Prog. Polym. Sci.* **2011**, *36*, 1415.
- [3] K. Jayaraman, M. Kotaki, Y. Z. Zhang, X. M. Mo, S. Ramakrishna, *J. Nanosci. Nanotechnol.* **2004**, *4*, 52.
- [4] Q. P. Pham, U. Sharma, A. G. Mikos, *Tissue Eng.* **2006**, *12*, 1197.
- [5] J. T. Chen, C. S. Hsu, *Polym. Chem.* **2011**, *2*, 2707.
- [6] A. Greiner, J. H. Wendorff, A. L. Yarin, E. Zussman, *Appl. Microbiol. Biotechnol.* **2006**, *71*, 387.
- [7] N. Haberkorn, M. C. Lechmann, B. H. Sohn, K. Char, J. S. Gutmann, P. Theato, *Macromol. Rapid Commun.* **2009**, *30*, 1146.
- [8] L. J. Pan, H. Qiu, C. M. Dou, Y. Li, L. Pu, J. B. Xu, Y. Shi, *Int. J. Mol. Sci.* **2010**, *11*, 2636.
- [9] C. R. Martin, *Accounts Chem. Res.* **1995**, *28*, 61.
- [10] L. J. Xue, A. Kovalev, F. Thole, G. T. Rengarajan, M. Steinhart, S. N. Gorb, *Langmuir* **2012**, *28*, 10781.
- [11] Y. J. Jang, Y. H. Jang, M. Steinhart, D. H. Kim, *Chem. Commun.* **2012**, *48*, 507.
- [12] D. Chen, W. Zhao, D. G. Wei, T. P. Russell, *Macromolecules* **2011**, *44*, 8020.
- [13] H. Duran, M. Steinhart, H. J. Butt, G. Floudas, *Nano Lett.* **2011**, *11*, 1671.
- [14] M. C. Garcia-Gutierrez, A. Linares, J. J. Hernandez, D. R. Rueda, T. A. Ezquerra, P. Poza, R. J. Davies, *Nano Lett.* **2010**, *10*, 1472.
- [15] J. Martin, J. Maiz, J. Sacristan, C. Mijangos, *Polymer* **2012**, *53*, 1149.
- [16] S. L. Mei, X. D. Feng, Z. X. Jin, *Macromolecules* **2011**, *44*, 1615.
- [17] M. Steinhart, S. Senz, R. B. Wehrspohn, U. Gosele, J. H. Wendorff, *Macromolecules* **2003**, *36*, 3646.
- [18] P. Dobriyal, H. Q. Xiang, M. Kazuyuki, J. T. Chen, H. Jinnai, T. P. Russell, *Macromolecules* **2009**, *42*, 9082.
- [19] V. M. Cepak, C. R. Martin, *Chem. Mat.* **1999**, *11*, 1363.
- [20] G. J. Song, X. L. She, Z. F. Fu, J. J. Li, *J. Mater. Res.* **2004**, *19*, 3324.
- [21] J. T. Chen, K. Shin, J. M. Leiston-Belanger, M. F. Zhang, T. P. Russell, *Adv. Funct. Mater.* **2006**, *16*, 1476.
- [22] S. Schlitt, A. Greiner, J. H. Wendorff, *Macromolecules* **2008**, *41*, 3228.
- [23] X. D. Feng, Z. X. Jin, *Macromolecules* **2009**, *42*, 569.
- [24] M. Steinhart, R. B. Wehrspohn, U. Gosele, J. H. Wendorff, *Angew. Chem.-Int. Edit.* **2004**, *43*, 1334.
- [25] M. Steinhart, J. H. Wendorff, A. Greiner, R. B. Wehrspohn, K. Nielsch, J. Schilling, J. Choi, U. Gosele, *Science* **2002**, *296*, 1997.
- [26] M. F. Zhang, P. Dobriyal, J. T. Chen, T. P. Russell, J. Olmo, A. Merry, *Nano Lett.* **2006**, *6*, 1075.
- [27] T. C. Wang, H. Y. Hsueh, R. M. Ho, *Chem. Mat.* **2010**, *22*, 4642.
- [28] P. G. De Gennes, *Rev. Mod. Phys.* **1985**, *57*, 827.
- [29] R. Fondecave, F. B. Wyart, *Europhys. Lett.* **1997**, *37*, 115.
- [30] T. Young, *Philos. Trans. R. Soc.* **1805**, *95*, 65.
- [31] C. W. Lee, T. H. Wei, C. W. Chang, J. T. Chen, *Macromol. Rapid Commun.* **2012**, *33*, 1381.
- [32] J. T. Chen, W. L. Chen, P. W. Fan, *ACS Macro Lett.* **2012**, *1*, 41.
- [33] J. T. Chen, D. Chen, T. P. Russell, *Langmuir* **2009**, *25*, 4331.
- [34] H. Q. Xiang, K. Shin, T. Kim, S. I. Moon, T. J. McCarthy, T. P. Russell, *Macromolecules* **2004**, *37*, 5660.
- [35] P. G. de Gennes, F. Brochard-Wyart, D. Quere, *Capillarity and Wetting Phenomena*, Springer, New York **2004**.
- [36] J. T. Chen, M. F. Zhang, T. P. Russell, *Nano Lett.* **2007**, *7*, 183.
- [37] D. Chen, J. T. Chen, E. Glogowski, T. Emrick, T. P. Russell, *Macromol. Rapid Commun.* **2009**, *30*, 377.
- [38] B. A. Miller-Chou, J. L. Koenig, *Prog. Polym. Sci.* **2003**, *28*, 1223.